

Applications of nuclear reactions calculations: Elastic scattering: the optical model

Antonio M. Moro



Universidad de Sevilla, Spain

Material available at: <https://github.com/ammoro/padova>

Recommended bibliography

- G.R. Satchler, *Introduction to nuclear reactions*, Macmillan (1990)
- G.R. Satchler, *Direct Nuclear Reactions*, Oxford University Press (1983)
- N. Glendenning, *Direct Nuclear Reactions*, World Scientific (2004)
- I.J. Thompson and F.M. Nunes, *Nuclear Reactions for Astrophysics*, Cambridge University Press (2009)
- A.M.M., *Models for nuclear reactions with weakly bound systems*, Proceedings of the International School of Physics Enrico Fermi Course 201 “Nuclear Physics with Stable and Radioactive Ion Beams” (<https://arxiv.org/abs/1807.04349>).



Modelling nuclear reactions

Why reaction theory is important?

- Many physical processes occurring spontaneously in nature (e.g. stars) or artificially (e.g. nuclear reactor) involve nuclear reactions. We need theoretical tools to evaluate their rates and cross sections.
- Reaction theory provides the necessary framework to extract meaningful **structure** information from measured **cross sections** and also permits the understanding of the **dynamics** of nuclear collisions.
- The many-body scattering problem is not solvable in general, so specific models tailored to specific types of reactions are used (**elastic**, **breakup**, **transfer**, **knockout**...) each of them emphasizing some particular degrees of freedom.
- In particular, exotic nuclei close to driplines are usually weakly-bound and **breakup** (coupling to the continuum) is important and must be taken into account in the reaction model.

Direct versus compound reactions

DIRECT: elastic, inelastic, transfer,...

- “fast” collisions (10^{-21} s).
- only a few modes (degrees of freedom) involved
- small momentum transfer
- angular distribution asymmetric about $\pi/2$ (forward peaked)

COMPOUND: complete, incomplete fusion.

- “slow” collisions ($10^{-18} - 10^{-16}$ s).
- many degrees of freedom involved
- large amount of momentum transfer
- “loss of memory” \Rightarrow dominated by statistical decay of emitted particles; almost forward/backward symmetric distributions (in CM)

Examples of direct and compound nucleus reactions

$$a + A \rightarrow b + B + Q \quad Q = (M_a + M_A - M_b - M_B)c^2 \text{ (energy released)}$$

- Elastic scattering:** $b = a, B = A$ ($Q = 0$)

E.g.: $\alpha + {}^{197}\text{Au} \rightarrow \alpha + {}^{197}\text{Au}$

- Inelastic scattering:** $b = a, B = A^*$ ($Q < 0$)

E.g.: $\alpha + {}^{197}\text{Au} \rightarrow \alpha + {}^{197}\text{Au}^*$

- Rearrangement or transfer:** $b \neq a, B \neq A$ Q positive or negative

E.g.: $d + {}^{208}\text{Pb} \rightarrow p + {}^{209}\text{Pb}$

- Breakup:** $a = b + x \Rightarrow a + A \rightarrow b + x + A$ ($Q < 0$)

E.g.: $d + {}^{208}\text{Pb} \rightarrow p + n + {}^{208}\text{Pb}$

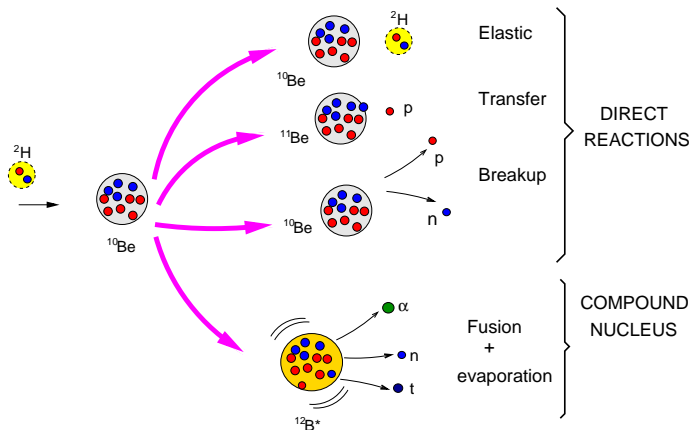
- Fusion:** reaction occurs via the formation of an intermediate compound nucleus:

$$a + B \rightarrow C^* \rightarrow b + B$$

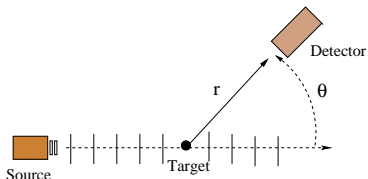
A special case is that of **capture** reactions ($b = \gamma$):

E.g.: $p + {}^{197}\text{Au} \rightarrow {}^{198}\text{Hg}^* \rightarrow \gamma + {}^{198}\text{Hg}_{\text{g.s.}}$

Example: the $d+^{10}\text{Be}$ reaction



Experimental cross section

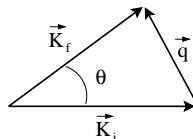
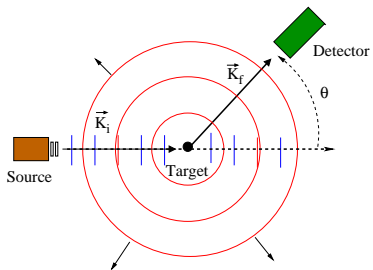


$$\Delta I = I_0 n_t \frac{d\sigma}{d\Omega} \Delta\Omega$$

- $\Delta\Omega$: solid angle of detector ($=\Delta A/r^2$)
- ΔI : detected particles per unit time in $\Delta\Omega$ (s^{-1})
- I_0 : incident particles per unit time and unit area ($s^{-1}L^{-2}$)
- n_t : number of target nuclei within the beam
- $d\sigma/d\Omega$: differential cross section (L^2)

$$\frac{d\sigma}{d\Omega} = \frac{\text{flux of scattered particles through } dA = r^2 d\Omega}{\text{incident flux}}$$

The scattering wavefunction



Among the many mathematical solutions of $[H - E]\Psi = 0$ we are interested in those behaving asymptotically as:

$$\Psi_{\mathbf{K}_\alpha}^{(+)} \rightarrow \Phi_\alpha(\xi_\alpha) e^{i\mathbf{K}_\alpha \cdot \mathbf{R}_\alpha} + (\text{outgoing spherical waves in } \alpha, \beta, \gamma, \dots)$$

where

- α denotes the incident channel and β, γ, \dots other (non-elastic channels)
- $\Phi_\alpha(\xi_\alpha)$ internal state of projectile+target in channel α

Scattering amplitude and cross sections

Asymptotically, when the projectile and target are well far apart,

$$\Psi_{\mathbf{K}_\alpha}^{(+)} \xrightarrow{R_\alpha \gg} \Phi_\alpha(\xi_\alpha) e^{i\mathbf{K}_\alpha \cdot \mathbf{R}_\alpha} + \Phi_\alpha(\xi_\alpha) f_{\alpha,\alpha}(\theta) \frac{e^{iK_\alpha R_\alpha}}{R_\alpha} \quad (\text{elastic})$$

$$+ \sum_{\alpha' \neq \alpha} \Phi_{\alpha'}(\xi_\alpha) f_{\alpha',\alpha}(\theta) \frac{e^{iK_{\alpha'} R_\alpha}}{R_\alpha} \quad (\text{inelastic})$$

$$\Psi_{\mathbf{K}_\alpha}^{(+)} \xrightarrow{R_\beta \gg} \sum_{\beta} \Phi_{\beta}(\xi_\beta) f_{\beta,\alpha}(\theta) \frac{e^{iK_\beta R_\beta}}{R_\beta} \quad (\text{transfer})$$

where the function $f_{\beta,\alpha}$ modulating the outgoing waves is called **scattering amplitude**

Cross sections:

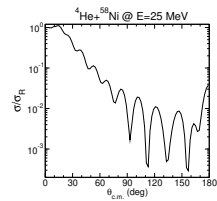
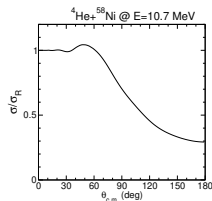
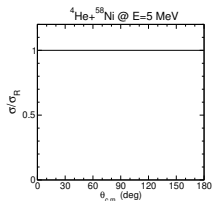
$$\left(\frac{d\sigma}{d\Omega} \right)_{\alpha \rightarrow \beta} = \frac{\mu_\alpha}{\mu_\beta} \frac{K_\beta}{K_\alpha} |f_{\beta,\alpha}(\theta)|^2$$

$$E = \frac{\hbar^2 K_\alpha^2}{2\mu_\alpha} + \varepsilon_\alpha = \frac{\hbar^2 K_\beta^2}{2\mu_\beta} + \varepsilon_\beta$$

Single-channel approach to elastic scattering: the optical model

The optical model

- Elastic scattering angular distributions exhibit a large variety of patterns depending on the colliding system and energy.



- The goal of the **optical model** is to describe these features by using an effective potential (optical potential)
- In general, the optical potential contains an **imaginary** part which is meant to account for **absorptive (nonelastic)** processes.

Elastic scattering in the optical model (no spin case)

- Effective Hamiltonian:

$$H = T_{\mathbf{R}} + U(\mathbf{R}) \quad (U(\mathbf{R}) \text{ complex!})$$

- Schrödinger equation:

$$[T_{\mathbf{R}} + U(\mathbf{R}) - E_{\alpha}] \chi_0^{(+)}(\mathbf{K}, \mathbf{R}) = 0 \quad (E_{\alpha} = \text{incident energy in CM})$$

- Boundary condition: Plane wave plus spherical wave, multiplied by the scattering amplitude $f(\theta, \phi)$:

$$\chi_0^{(+)}(\mathbf{K}, \mathbf{R}) \rightarrow e^{i\mathbf{K} \cdot \mathbf{R}} + f(\theta, \phi) \frac{e^{iKR}}{R} \quad K = \frac{\sqrt{2\mu E_{\alpha}}}{\hbar}$$

- Elastic differential cross section:

$$\frac{d\sigma}{d\Omega} = |f(\theta, \phi)|^2$$

Partial wave decomposition

- For a central potential [$U(\mathbf{R}) = U(R)$], the scattering wavefunction can be expanded in spherical harmonics:

$$\chi_0^{(+)}(\mathbf{K}, \mathbf{R}) = \frac{1}{KR} \sum_{\ell} i^{\ell} \chi_{\ell}(K, R) (2\ell + 1) P_{\ell}(\cos \theta) \quad (\theta = \text{scattering angle})$$

- The radial wavefunctions $\chi_{\ell}(K, R)$ satisfy the equation:

$$\left[-\frac{\hbar^2}{2\mu} \frac{d^2}{dR^2} + \frac{\hbar^2}{2\mu} \frac{\ell(\ell + 1)}{R^2} + U(R) - E_0 \right] \chi_{\ell}(K, R) = 0.$$

- For a zero potential ($U = 0$) the solution is just the plane wave:

$$\chi_0^{(+)}(\mathbf{K}, \mathbf{R}) = e^{i\mathbf{K}\mathbf{R}} \quad \Rightarrow \quad \chi_{\ell}(K, R) \rightarrow F_{\ell}(KR) = \frac{i}{2} [H_{\ell}^{(-)}(KR) - H_{\ell}^{(+)}(KR)]$$

$$\text{where:} \quad F_{\ell}(KR) \rightarrow \sin(KR - \ell\pi/2) \quad ; \quad H_{\ell}^{(\pm)}(KR) \rightarrow e^{\pm i(KR - \ell\pi/2)}$$

Non-zero potential: asymptotic behaviour

- For $R \gg \Rightarrow U(R) = 0 \Rightarrow \chi_\ell(K, R)$ will be a combination of F_ℓ and G_ℓ

$$F_\ell(KR) \rightarrow \sin(KR - \ell\pi/2) \quad G_\ell(KR) \rightarrow \cos(KR - \ell\pi/2)$$

or their *outgoing/ingoing* combinations:

$$H^{(\pm)}(KR) \equiv G_\ell(KR) \pm iF_\ell(KR) \rightarrow e^{\pm i(KR - \ell\pi/2)}$$

- The specific combination is determined by the physical boundary condition:

$$\begin{array}{rclcl}
 \chi_0^{(+)}(\mathbf{K}\mathbf{R}) & \rightarrow & e^{i\mathbf{K}\cdot\mathbf{R}} & + & f(\theta) \frac{e^{iKR}}{R} \\
 \Downarrow & & \Downarrow & & \Downarrow \\
 U = 0 \quad \chi_\ell(KR) & \rightarrow & F_\ell(KR) & + & 0 \\
 U \neq 0 \quad \chi_\ell(KR) & \rightarrow & F_\ell(KR) & + & T_\ell H^{(+)}(KR)
 \end{array}$$

 The coefficients T_ℓ are to be determined by numerical integration.

Numerical integration of Schrodinger equation

- ① Fix a *matching radius*, R_m , such that $U(R_m) \approx 0$
- ② Integrate $\chi_\ell(R)$ from $R = 0$ up to R_m , starting with the condition:

$$\lim_{R \rightarrow 0} \chi_\ell(K, R) = 0$$

- ③ At $R = R_m$ impose the boundary condition:

$$\begin{aligned} \chi_\ell(K, R) &\rightarrow F_\ell(KR) + T_\ell H_\ell^{(+)}(KR) \\ &= \frac{i}{2} [H_\ell^{(-)}(KR) - S_\ell H_\ell^{(+)}(KR)] \end{aligned}$$

👉 $S_\ell = 1 + 2iT_\ell = \mathbf{S}\text{-matrix}$

- ④ **Phase-shifts:**

$$S_\ell \equiv e^{i2\delta_\ell}$$

$$T_\ell = e^{i\delta_\ell} \sin(\delta_\ell)$$

$$\chi_\ell(K, R) \rightarrow e^{i\delta_\ell} \sin(KR + \delta_\ell - \ell\pi/2)$$

The scattering amplitude

- Replace the asymptotic $\chi_\ell(K, R)$ in the general expansion:

$$\begin{aligned}\chi_\ell(K, R) &= \frac{1}{KR} \sum_{\ell} i^\ell (2\ell + 1) \chi_\ell(K, R) P_\ell(\cos \theta) \\ &\rightarrow \frac{1}{KR} \sum_{\ell} i^\ell (2\ell + 1) \left[F_\ell(KR) + T_\ell H^{(+)}(KR) \right] P_\ell(\cos \theta)\end{aligned}$$

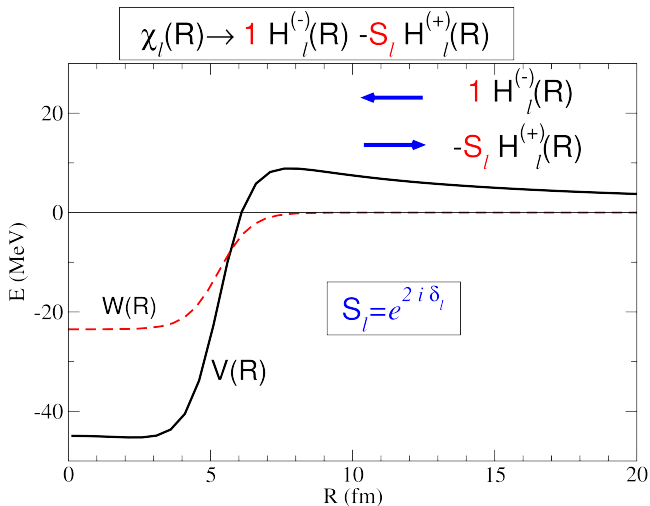
- The scattering amplitude is the coefficient of e^{iKR}/R of $\chi^{(+)}(K, R)$:

$$\begin{aligned}f(\theta) &= \frac{1}{K} \sum_{\ell} (2\ell + 1) T_\ell P_\ell(\cos \theta) \\ &= \frac{1}{2iK} \sum_{\ell} (2\ell + 1) (S_\ell - 1) P_\ell(\cos \theta).\end{aligned}$$

- Elastic differential cross section:

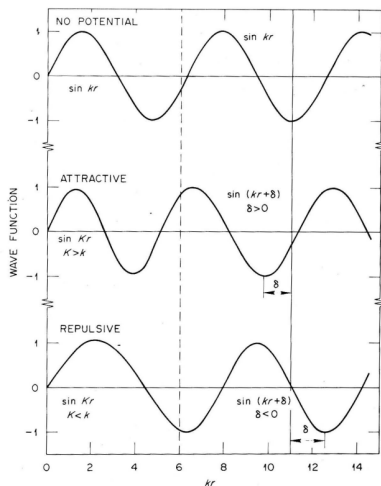
$$\frac{d\sigma}{d\Omega} = |f(\theta)|^2$$

Interpretation of the S-matrix (single-channel case)



Interpretation of the S-matrix (single-channel case)

- S_ℓ = coefficient of the outgoing wave for partial wave ℓ .
- For $U = 0 \Rightarrow S_\ell = 1$
- $|S_\ell|^2$ is the *survival* probability for the partial wave ℓ :
 - U real $\Rightarrow |S_\ell| = 1 \Rightarrow \delta_\ell$ real
 - U complex $\Rightarrow |S_\ell| < 1 \Rightarrow \delta_\ell$ complex
- For $\ell \gg \Rightarrow S_\ell \rightarrow 1$
- Sign of $Re[\delta]$:
 - $Re[\delta] > 0 \Rightarrow$ attractive potential
 - $Re[\delta] < 0 \Rightarrow$ repulsive potential
 - $Re[\delta] = 0$ ($S_\ell = 1$) \Rightarrow no potential ($U(R) = 0$)

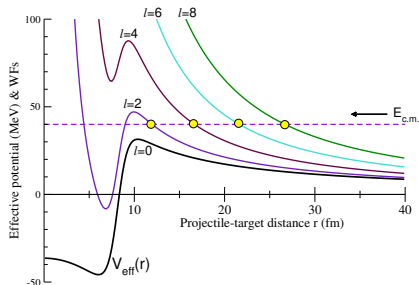


Interpretation of the S-matrix (single-channel case)

Effective potential:

$$V_{\text{eff}}(r) = V_N(r) + V_C(r) + \frac{\ell(\ell + 1)\hbar^2}{2\mu r^2}$$

As the ℓ value increases, so does the centrifugal potential, preventing the projectile from approaching the target and hence reducing the effect of the nuclear (real and imaginary) potentials. Thus, for $\ell \gg \Rightarrow S_\ell \rightarrow 1$



Coulomb plus nuclear case

Radial equation:

$$\left[\frac{d^2}{dR^2} + K^2 - \frac{2\eta K}{R} + \frac{2\mu}{\hbar^2} U(R) + \frac{\ell(\ell+1)}{R^2} \right] \chi_\ell(K, R) = 0$$

$$\eta = \frac{Z_p Z_t e^2}{4\pi\epsilon_0 \hbar v} = \frac{Z_p Z_t e^2 \mu}{4\pi\epsilon_0 \hbar^2 K}$$

(Sommerfeld parameter)

Asymptotic condition:

$$\chi_\ell^{(+)}(\mathbf{K}, \mathbf{R}) \rightarrow e^{i[\mathbf{K} \cdot \mathbf{R} + \eta \log(kR - \mathbf{K} \cdot \mathbf{R})]} + f(\theta) \frac{e^{i(KR - \eta \log 2KR)}}{R}$$

$$\begin{aligned} \chi_\ell(K, R) &\rightarrow e^{i\sigma_\ell} \left[F_\ell(\eta, KR) + T_\ell H_\ell^{(+)}(\eta, KR) \right] \\ &= \frac{i}{2} e^{i\sigma_\ell} \left[H_\ell^{(-)}(\eta, KR) - S_\ell H_\ell^{(+)}(\eta, KR) \right] \end{aligned}$$

- ☞ $\sigma_\ell(\eta)$ = Coulomb phase shift
- ☞ $F_\ell(\eta, KR)$ = regular Coulomb wave
- ☞ $H_\ell^{(\pm)}(\eta, KR)$ = outgoing/ingoing Coulomb wave

Coulomb plus nuclear case: scattering amplitude

Total scattering amplitude:

$$f(\theta) = f_C(\theta) + \frac{1}{2iK} \sum_{\ell} (2\ell + 1) e^{2i\sigma_{\ell}} (S_{\ell} - 1) P_{\ell}(\cos \theta)$$

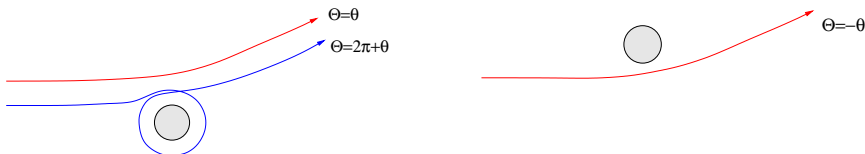
☞ $f_C(\theta)$ is the amplitude for pure Coulomb:

$$\frac{d\sigma_R}{d\Omega} = |f_C(\theta)|^2 = \frac{\eta^2}{4K^2 \sin^4(\frac{1}{2}\theta)} = \left(\frac{Z_p Z_t e^2}{16\pi\epsilon_0 E} \right)^2 \frac{1}{\sin^4(\frac{1}{2}\theta)}$$

Classical interpretation of elastic scattering

Deflection angle vs deflection function

- **Scattering angle:** Angle formed by the final direction and the initial direction.
 $0 \leq \theta \leq \pi$. It is the quantity observed experimentally in a scattering experiment.
- **Deflection angle:** Angle which is covered by the trajectory $\Theta = \pm\theta + 2n\pi$.
 Several deflection angles can correspond to the same scattering angle.



- ☞ For each impact parameter b there is a single value of the deflection angle Θ and of the scattering angle $\theta(b)$.
- ☞ For a given scattering angle θ there may be several trajectories, corresponding to different values of b .
- ☞ $\Theta = \theta > 0$ is a **near-side** trajectory (the projectile bypasses the target “near” the detector).
- ☞ $\Theta = -\theta < 0$ is a **far-side** trajectory (the projectile bypasses the target “far” from the detector).
- ☞ $\Theta = \pm\theta + 2\pi n$ are **orbiting** trajectories (the projectile “orbits” around the target).

Deflection function and classical cross section

- For a given projectile-target potential $V(r)$, the deflection function can be obtained for each impact parameter solving:

$$\Theta(b) = \pi - 2 \int_{r_0}^{\infty} \frac{b}{r^2} \frac{dr}{\sqrt{1 - \frac{V(r)}{E} - \frac{b^2}{r^2}}}$$

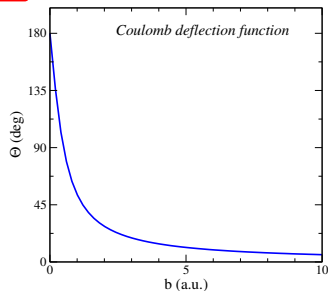
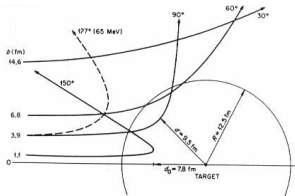
- The **classical scattering cross section** is a function of the deflection function (or scattering angle) according to:

$$\frac{d\sigma}{d\Omega} = \frac{b}{\sin(\theta)} \left| \frac{db}{d\theta} \right|$$

Classical deflection function for point Coulomb case

- For a point Coulomb potential, the deflection function is given analytically by:

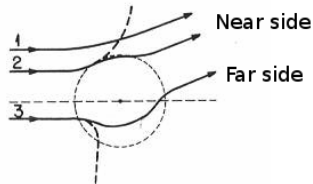
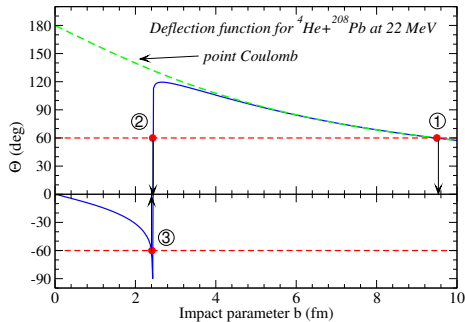
$$b = a_0 \cot\left(\frac{\theta}{2}\right)$$



- When b increases, for a given energy E , r_{CA} increases and θ decreases.
- When E increases, for a given b , r_{CA} decreases and θ decreases.

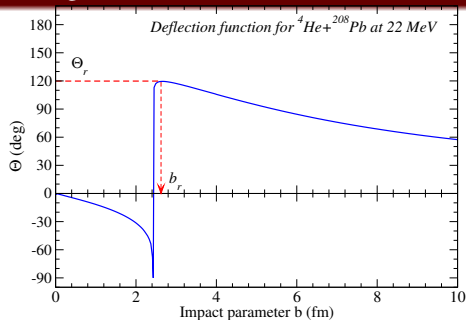
Coulomb + nuclear scattering: deflection function

☞ For large values of b , the scattering is Coulombic (the projectile does not feel the nuclear potential).



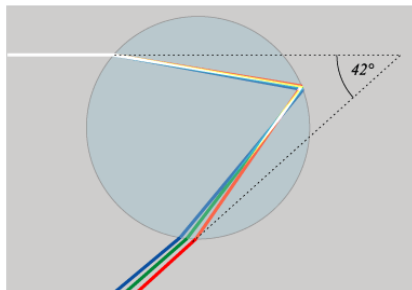
☞ For a given scattering angle θ there are in general 3 values of b contributing to this angle. (1) is the Coulomb trajectory, (2) is the nuclear near-side trajectory, and (3) is the nuclear far-side trajectory.

Coulomb + nuclear scattering: Rainbow

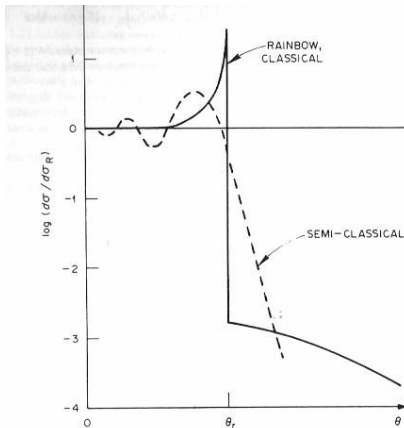


- ☞ The deflection function has a maximum at $b = b_r \rightarrow \Theta_r$ (rainbow angle)
- ☞ For $b = b_r$: $\frac{d\Theta}{db} = 0 \Rightarrow \frac{db}{d\Theta} = 0 \Rightarrow \frac{d\sigma}{d\Omega} \rightarrow \infty$
- ☞ In the vicinity of b_r , many trajectories give approximately the same scattering angle (Θ_r)
- ☞ For angles greater than the rainbow ($\theta > \Theta_r$), neither the Coulomb trajectories nor the nuclear nearside trajectories contribute to the cross section so, classically, there is a sharp decrease in the differential cross section for ($\theta > \Theta_r$). This is the “shadow region”.

Atmospheric rainbow



Coulomb + nuclear scattering: undulatory effects



✎ In a treatment beyond the classical limit, several trajectories may interfere, and the divergence at the rainbow is smoothed.

Elastic scattering phenomenology

Nucleus-nucleus scattering: Optical Potential

Optical potential: $\mathcal{V} \approx U(r) = U_{\text{nuc}}(r) + V_{\text{coul}}(r)$

- **Coulomb potential:** charge sphere distribution

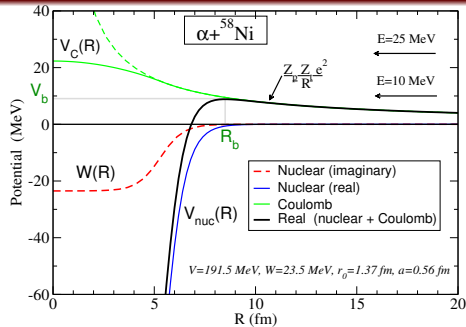
$$V_{\text{coul}}(r) = \begin{cases} \frac{Z_1 Z_2 e^2}{2R_c} \left(3 - \frac{r^2}{R_c^2} \right) & \text{if } r \leq R_c \\ \frac{Z_1 Z_2 e^2}{r} & \text{if } r \geq R_c \end{cases}$$

- **Nuclear potential (complex):** Eg. Woods-Saxon parametrization

$$U_{\text{nuc}}(r) = V(r) + iW(r) = -\frac{V_0(E)}{1 + \exp\left(\frac{r-R_V}{a_V}\right)} - i \frac{W_0(E)}{1 + \exp\left(\frac{r-R_W}{a_W}\right)}$$

- **Potential parameters:** 6, fitted to reproduce the elastic differential cross sections.
 - Depths $V_0(E)$, $W_0(E)$;
 - Radii $R_{V,W} = r_{V,W}(A_p^{1/3} + A_t^{1/3})$. $r_V \approx r_W \sim 1.1 - 1.4$ fm.
 - Difuseness $a_V \approx a_W \sim 0.5 - 0.7$ fm

Nucleus-nucleus scattering: The Coulomb barrier



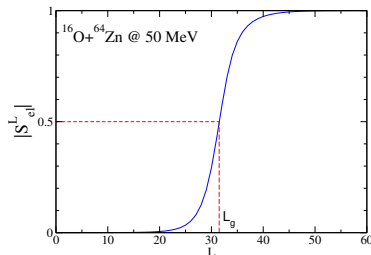
- The maximum of $V_N(r) + V_C(r)$ defines the Coulomb barrier. The radius of the barrier is R_b . The height of the barrier is $V_b = V_N(R_b) + V_C(R_b)$
- As a **rough approximation**,

$$R_b \simeq 1.44(A_p^{1/3} + A_t^{1/3}) \text{ fm}$$

$$V_b \simeq \frac{Z_p Z_t e^2}{4\pi\epsilon_0 R_b} \approx \frac{Z_p Z_t}{(A_p^{1/3} + A_t^{1/3})} [\text{MeV}]$$

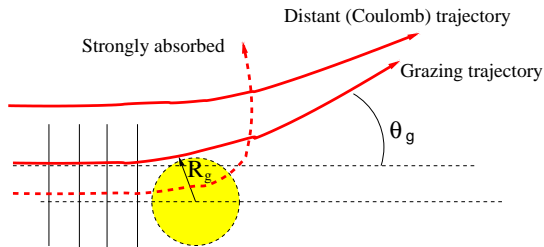
Nucleus-Nucleus Elastic scattering: Strong absorption

- The **nuclear attraction** is determined by the **real part** of the optical potential $V(r)$. Together with the Coulomb potential, determines the Coulomb barrier.
- The **absorption**, which corresponds to the removal of flux from the elastic channel, is determined by the **imaginary part** of the optical potential $W(r)$.
- Elastic scattering of heavy nuclei (beyond He) display strong absorption. One can define a **grazing angular momentum** (ℓ_g), such that:
 - $|S_\ell| \approx 0$ when $\ell \ll \ell_g$ and $|S_\ell| \rightarrow 1$ when $\ell \gg \ell_g$.
 - A convenient quantitative definition of the grazing angular momentum (ℓ_g) is provided by the condition $|S(\ell_g)| \simeq \frac{1}{2}$



Strong absorption: Classical interpretation

- The grazing angular momentum ℓ_g is associated to a **grazing distance** R_g , which is its distance of closest approach $R_g = a_0 + \sqrt{a_0^2 + (\ell_g + 1/2)^2/k^2}$.
- When Coulomb is weak (or absent): $kR_g \approx (\ell_g + 1/2)$
- The grazing distance $R_g \simeq (1.4 - 1.5)(A_p^{1/3} + A_t^{1/3})$ is approximately independent of the energy, so ℓ_g increases with energy.
- Angular momenta with $\ell < \ell_g$ are associated with trajectories which come inside R_g , and are strongly absorbed ($|S_\ell| \ll 1$).



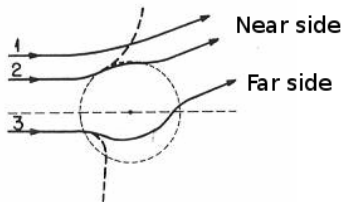
Near-side and far-side decomposition

For $\ell \gg 1$ and $\frac{1}{\ell + \frac{1}{2}} \lesssim \theta \lesssim \pi - \frac{1}{\ell + \frac{1}{2}}$

$$P_\ell(\cos \theta) \simeq \frac{e^{i((\ell + \frac{1}{2})\theta - \frac{\pi}{4})} - e^{-i((\ell + \frac{1}{2})\theta - \frac{\pi}{4})}}{\sqrt{2\pi(\ell + \frac{1}{2})\cos \theta}} \Rightarrow f(\theta) = f^{\text{far}}(\theta) + f^{\text{near}}(\theta)$$

Classically, the contributions would correspond to **near-side** and **far-side** trajectories:

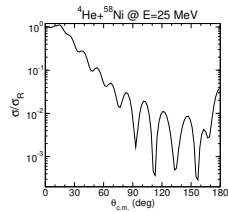
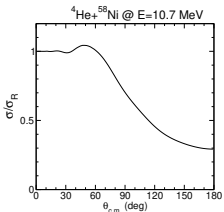
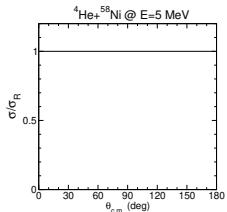
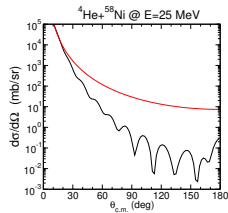
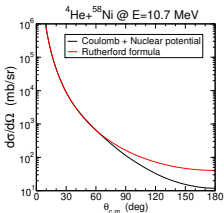
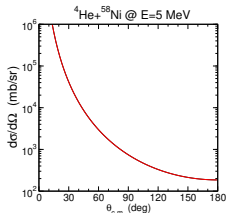
- ⇒ The repulsive Coulomb potential tends to deflect the trajectories outward from the target (**near-side** trajectories).
- ⇒ Nuclear attraction tends to bend the trajectories inwards (**far-side** trajectories).
- ⇒ Near- and far-side trajectories may give rise to the same scattering angle so, if their amplitudes are similar, interference effects will occur.



Patterns of elastic scattering: Energy dependence

- The semi-classical vs quantum character of the scattering can be given in terms of the Sommerfeld parameter: $\eta = \frac{Z_p Z_t e^2}{4\pi\epsilon_0 \hbar v}$
- The Coulomb vs nuclear relevance, in terms of the energy of the Coulomb barrier: $V_b \simeq \frac{Z_p Z_t}{A_p^{1/3} + A_t^{1/3}} \text{ [MeV]}$
- Three distinct patterns appear for the elastic cross sections
 - Nuclear relevant $E > V_b$, quantum $\eta \lesssim 1 \Rightarrow$ Fraunhofer scattering
 - Nuclear relevant $E > V_b$, semiclassical $\eta \gg 1 \Rightarrow$ Fresnel scattering
 - Coulomb-dominated $E < V_b \Rightarrow$ Rutherford scattering

Patterns of elastic scattering: $^4\text{He}+^{58}\text{Ni}$ example

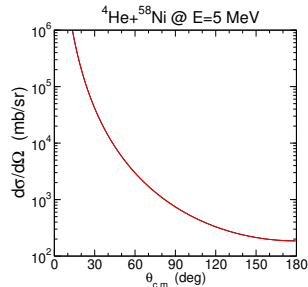
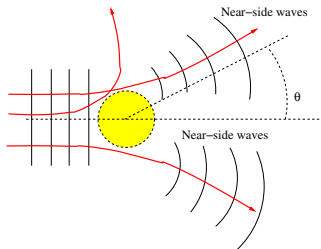


Rutherford scattering

Fresnel Scattering

Fraunhofer Scattering

Rutherford scattering

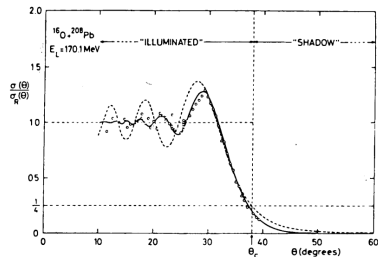
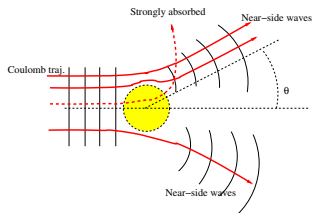


- Centre of mass energy below the Coulomb barrier ($E < V_b$): Nuclear potential does not affect the scattering.
- Analytical differential cross sections (same for classical and quantum!)

$$\frac{d\sigma}{d\Omega} = \left(\kappa \frac{Z_p Z_t e^2}{2E} \right)^2 \frac{1}{\sin^4(\theta/2)}$$

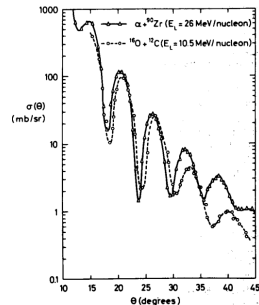
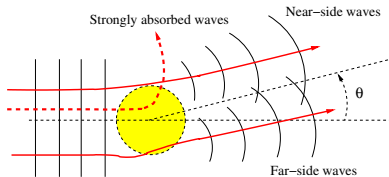
Fresnel scattering

- Analogous to light scattering from an object with size $R_g \gg \lambda$. Leads to $\eta \gg 1$.
- The grazing angular momentum (ℓ_g) determines a grazing angle (θ_g), such that $\ell_g = \eta \cot(\theta_g/2)$, and a grazing distance $R_g = \frac{a_0}{2} (1 + \sin(\theta_g/2)^{-1})$.
- Quarter-point recipe: $|S(\ell_g)| = 1/2$ implies $\sigma/\sigma_R(\theta_g) = 1/4$.
- Angular pattern divided in *illuminated* ($\theta < \theta_g$) and *shadow* ($\theta > \theta_g$) regions. Interference between pure Coulomb and near-side trajectories produce oscillations.



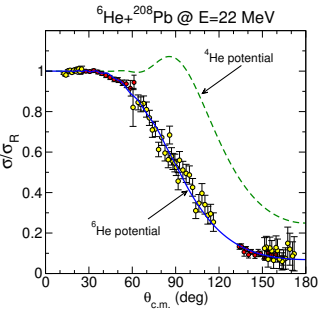
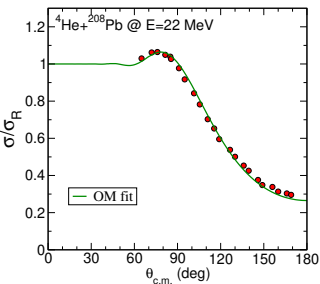
Fraunhofer scattering

- Analogous to the scattering of light by an object which has a size $R_g \simeq \lambda$
- Waves scattering from the the two sides interfere constructively or destructively, giving rise to a diffraction pattern of maxima and minima spaced by $\Delta\theta = \pi/\ell_g \approx \pi/kR_g$
- Since $\Delta\theta \sim 1/\sqrt{E}$, as energy increases, oscillating pattern compresses and more oscillations appear.



Elastic scattering of halo nuclei

How does the halo structure affect the elastic scattering?



- $^4\text{He} + ^{208}\text{Pb}$ shows typical Fresnel pattern and “standard” optical model parameters
- $^6\text{He} + ^{208}\text{Pb}$ shows a prominent reduction in the elastic cross section, suggesting that part of the incident flux goes to non-elastic channels (e.g. breakup, neutron transfer)